ELSEVIER

Biomaterials 22 (2001) 3155–3168

Biomaterials

www.elsevier.com/locate/biomaterials

Characterization of rat meningeal cultures on materials of differing surface chemistry

Michael E. Manwaring, Roy Biran, Patrick A. Tresco*

The Keck Center for Tissue Engineering, Department of Bioengineering, University of Utah, 20 South 2030 East Building 570, Room 108D, Salt Lake City, UT 84112-9458, USA

Received 20 October 2000; accepted 13 February 2001

Abstract

To better understand the interactions of cells derived from meningeal tissues with the surfaces of devices used for the treatment of central nervous system disorders, the behavior of primary postnatal day 1 rat meningeal cultures was evaluated on biomaterials of differing surface chemistry. Meningeal cultures in serum containing media were analyzed for attachment, spread cell area, proliferation, the production of extracellular matrix (ECM), and neuronal outgrowth. In general, both cell attachment as well as cell spread area decreased with increasing substrate hydrophobicity, whereas cell division as indicated by BrdU incorporation and time to confluence, was lower on the most hydrophobic materials. We suggest that such differences immediately after cell seeding were most likely mediated by differences in surface adsorption of proteins. In longer-term experiments, most of the materials were colonized by meningeal cultures irrespective of surface chemistry, and all cultures were equally inhibitory to neuronal outgrowth suggesting that over time, cells can modify the substrate perhaps by secretion of extracellular matrix molecule proteins. Our data suggests that cell type-specific differences in response to different biomaterials may play an important role in determining the ultimate nature and composition of the CNS at the host–biomaterial interface.

Keywords: Meningeal cells; Synthetic materials; Cell adhesion; Cell surface area; DNA synthesis

1. Introduction

A variety of devices are being investigated for treating central nervous system (CNS) disorders including drainage shunts, catheters, dural substitutes, stimulating and recording electrodes, cell encapsulation devices and nerve guidance channels. Regardless of the application, currently available biomaterials elicit a similar inflammatory and scarring response that includes macrophages, microglia, endothelia, astrocytes, fibroblasts, and meningeal cells [1–5].

The meninges form a protective sheathing structure surrounding the brain and spinal cord composed of the outermost dura mater, the intermediate arachnoid mater, and the internal pia mater [6]. The cells of the meninges contain tight junctions [7–9], and establish a glia limitans with the interdigitating astrocytic endfeet of the underlying brain tissue [4]. They secrete an abundance of extracellular matrix (ECM) and have been proposed to serve blood brain barrier functions [8,10,11].

Implantation of biomaterials into the brain and spinal cord disrupts the integrity of the meninges, eliciting a scarring response characterized by increased matrix production as well as division and migration of meningeal cells within the lesion cavity and surrounding the implant interface [1–3,12,13]. Reactive cell colonization of materials implanted in the CNS is known to alter device performance by blocking flow in drainage shunts, catheters, cannulas, and infusion pumps [14–16], creating impedance barriers to recording electrodes [17,18], and perhaps fouling dialysis probes and cell encapsulation membranes. In addition, normal wound-healing processes can inhibit neurite extension in nerve guidance and regeneration devices [3,19–21].

At present little is known about the response of the cells of the meninges to biomaterials used in CNS applications. Previously, we examined the interactions of astrocytes, which are known to be a major component of the CNS scar, on surfaces of differing chemistry [22]. To build upon this work and perhaps

*Corresponding author. Tel.: +1-801-581-8873; fax: +1-801-585-5151.
E-mail address: patrick.tresco@m.cc.utah.edu (P.A. Tresco).

0142-9612/01/$ - see front matter
PII: S0142-9612(01)00068-0

shed light on the impact of normal CNS wound healing on device performance, we examined the interactions of meningeal cultures using model surfaces of differing chemistry. For our studies, we developed and characterized a meningeal culture system derived from the meninges of postnatal rat brains, and evaluated its cellular composition over time by counting the relative abundance of astrocytes, macrophages, microglia, endothelial cells, smooth muscle cells and neurons. Meningeal cultures were then plated on biomaterial surfaces in dilute serum-containing medium to study cell–material interactions. We report on differences in cellular composition, cell adhesion, cell spread area, cell proliferation, the deposition of extracellular matrix with time in culture, and compare the behavior of meningeal cultures to that of astrocyte cultures grown on similar surfaces.

2. Materials and methods

2.1. Meningeal culture preparation

Meningeal tissue was carefully peeled from the surface of postnatal day 1 rat brains under a stereomicroscope, and collected in a droplet of L15 medium (Gibco). The dissected tissue was minced, and digested in 0.5% collagenase (Sigma) in DMEM for 30 min. Following centrifugation at 600 *g* for 5 min, the supernatant was removed, and resuspended in a solution of 0.06% trypsin/EDTA (Sigma) for 30 min. The resulting solution was centrifuged again, and resuspended in 0.1% DNAse (Worthington) in DMEM-FBS (DMEM with 10% fetal bovine serum, 2 mM glutamine, and 25 μg/ml gentamicin). The solution was sequentially titurated through a fire-polished pasteur pipette, and a 1 cm^3 syringe with 21 and 23 gauge needles. The resulting cell suspension was centrifuged for 5 min at 1000 *g*, resuspended in DMEM-FBS, counted using a hemacytometer, and plated onto coverslips.

2.2. Cellular composition of the meningeal cultures

Although meningeal cells stain positively for a variety of cytoskeletal and ECM proteins, including vimentin and fibronectin, there are no available meningeal specific markers [23–25]. To determine the types and quantity of cells present in the meningeal cultures, known cell-specific markers were used. Sterilized tissue culture grade plastic (TCP; Sarstedt), glass, and polymeric thin-film coverslips, were placed into 24 well plates (ultralow protein binding; Costar) containing 0.5 ml of DMEM-FBS. Approximately 5000 meningeal cells were plated on each coverslip, incubated at 37°C, fixed after 24 h and upon reaching confluence. Cell populations at two time points were characterized using immunofluorescence with cell-specific markers: neuronal cells were identified with βIII tubulin (mouse IgG2b; Sigma); endothelia with rat endothelial cell antigen (RECA-1, mouse IgG1; Serotec) [26]; smooth muscle cells with desmin (mouse IgG1; Chemicon) [27]; astrocytes with GFAP (bovine IgG; Dako); and, macrophages and microglia by ED-1 (mouse IgG1; Serotec) [28].

Cells were fixed in 4% (w/v) paraformaldehyde, permeabilized with 0.5% Triton in PBS for 2 min for intracellular antibodies, and treated by sequential 1 h steps of primary and secondary antibodies. Primary antibodies were diluted 1 : 1000 in Hank's balanced salt solution containing 0.05% (w/v) sodium azide and 5% heat-inactivated donor calf serum (Gibco), buffered to pH 7.4 with HEPES (Sigma). Secondary antibodies were diluted 1 : 200 in Hanks balanced salt solution, which included goat anti-mouse IgG2b FITC (Southern Biotechnology Associates) for βIII tubulin, or goat anti-rabbit IgG(H + L) Alexa 594 (Molecular Probes) for GFAP, or goat anti-mouse IgG1 Alexa 594 (Molecular Probes) for desmin, RECA-1, and ED-1. All cells were counterstained by the nuclear dye 4′,6-diamidino-2-phenylindole, dihydrochloride (DAPI; molecular probes). Following a final wash in distilled water, the various materials were placed on a glass slide, coated with fluoromount-G (Southern Biotechnology Associates) and covered with a glass coverslip. Cells were viewed using a Nikon Eclipse E600 microscope equipped with phase-contrast optics, epifluorescent illumination, and selective filters. The percentage of positively stained cells for each cell marker was determined at 24 h and at confluence by counting 21 predetermined fields from each of two coverslips.

2.3. Co-culture of neurons on confluent meningeal cultures

Confluent meningeal cultures were examined for their ability to support neurite outgrowth of peripheral and central neurons. Cells derived from the meninges were isolated and plated at a density of approximately 5000 cells per coverslip as described above. Meningeal cultures were grown to confluence, then co-cultured with either dorsal root ganglion (DRG) neurons, or cerebellar granule neurons (CGN), in serum containing media. DRG neurons were isolated from postnatal day 1 rat pups, while CGNs were derived from postnatal day 8 rat pups, as described previously [29]. Co-cultures were fixed after 24 h in 4% paraformaldehyde, digital images were captured, and neurite outgrowth was measured using computer-assisted image analysis. Neurite outgrowth was estimated by measuring the longest process from each cell body. For control model surfaces, DRG neurons were cultured on laminin-coated (20 μg/ml; Gibco) TCP coverslips, and CGNs were cultured on L1 (100 μg/ml; gift from Acorda Therapeutics Inc.,

Hawthorne, NY) adsorbed to unmodified polystyrene. Neurite outgrowth on the meningeal monolayer is reported as the percentage of outgrowth on the relative model surfaces.

2.4. Biomaterial preparation and characterization

Polymer-coated glass coverslips were produced from polymer solutions using a spin coating apparatus. Prior to polymer application, the coverslips (13 mm diameter; Baxter) were cleaned by sequential rinses of distilled water, 95% ethanol, distilled water, and acetone, then blown dry with filtered nitrogen. The following polymer solutions were used: 10% (w/v) cellulose acetate (CA) dissolved in acetone, 6% (w/v) polyacrylonitrile-polyvinyl chloride (PAN-PVC) dissolved in DMF/acetone(1 : 1), 10% (w/v) polyether sulfone (PES) dissolved in NNP, 5% (w/v) polyethylene vinyl acetate (PEVAC) dissolved in methylene chloride, 5% (w/v) polypropylene (PP) dissolved in hot decalin, 15% (w/v) polystyrene (PS) dissolved in toluene, and 2% (w/v) Tecoflex (TECO) dissolved in methylene chloride. A drop of solution was placed in the center of the coverslip, then spun to create a thin-film covering. Spin speed and duration for each solution were optimized for uniform coating. The thin-film coverslips were dried overnight at 70°C to evaporate the solvents. Untreated glass (Baxter) and TCP coverslips were used as comparative surfaces. All coverslips were sterilized in 70% ethanol and rinsed with double distilled water prior to cell culture. Thin films were analyzed by contact angle using the sessile drop method and characterized by attenuated total reflection-fourier transform infrared (ATR-FTIR) spectroscopy.

2.5. Adhesion, cell spread area, surface coverage, and proliferation

For measurement of cell adhesion, cell spread area, and proliferation, approximately 5000 cells were plated on the sterilized thin-film coverslips, as described above. Cells were fixed with 4% paraformaldehyde at 24 h for cell adhesion and cell spread area, and visualized using rhodamine phalloidin (Molecular Probes) counterstained by DAPI for examination of the actin cytoskeleton, and quantification of cell number. Representative images were captured using a digital camera, and area measurements were calculated using computer-assisted image analysis. Cell surface coverage was measured by dividing the total cell area by the area of the field of view. Cells were treated with 10 μM 5-bromodeoxyuridine (BrdU) for 4 h prior to fixation with 4% paraformaldehyde at 48 h for estimation of cell proliferation as measured by the percentage of cells undergoing DNA synthesis [30].

2.6. Expression of extracellular matrix

Approximately 5000 cells were plated onto each coverslip, as described above. Cells were fixed with 4% paraformaldehyde at three time points, 48 h after plating, at confluence, and 7 days after reaching confluence. Indirect immunohistochemistry was used to analyze the expression of cellular fibronectin (mouse IgM; Sigma), type I collagen (rabbit IgG; Chemicon), and chondroitin sulfate proteoglycan (CS56, mouse IgM; Sigma). The method was performed as previously described, and representative images were captured with a digital camera. Secondary antibodies included goat anti-rabbit IgG(H + L) Alexa 594 (Molecular Probes) for collagen, and goat anti-mouse IgM Texas Red (Southern Biotechnology Associates) for cellular fibronectin and CS56.

2.7. Statistical analysis

Data for cell populations on the different materials, including cellular composition, cell attachment, cell spread area, BrdU incorporation, and neuronal outgrowth were analyzed by ANOVA using Tukey's method for multiple comparisons with a p value <0.05 defined as significant. All data are reported as the mean $\pm$ the standard error of the mean.

3. Results

3.1. Composition of meningeal cultures on TCP

To establish a meningeal culture system, we plated cells derived from the meninges on TCP coverslips in dilute serum-containing medium. Cells attached to the tissue culture treated surfaces, and readily reached confluence. We evaluated the cellular composition of the meningeal cultures on TCP 24 h after plating and upon reaching confluence to determine the amounts and the relative abundance of the different types of cells present in the meningeal culture. As there are no available meningeal cell-specific markers, the cultures were characterized for the presence of known cell types contained within the extracted meningeal tissue, including neurons, endothelial cells, smooth muscle cells, astrocytes, macrophages and microglia. All vimentin-positive cells that did not stain for known markers were assumed to be meningeal fibroblasts. Fig. 1 shows the percentage of each cell type present on TCP 24 h after plating and at confluence. At 24 h the bulk of the culture was composed of fibroblasts, as less than 14% of the cells labeled positively for various cell-type-specific markers.

Of the labeled cell types, ED-1 positive macrophages and microglia formed the largest group, at

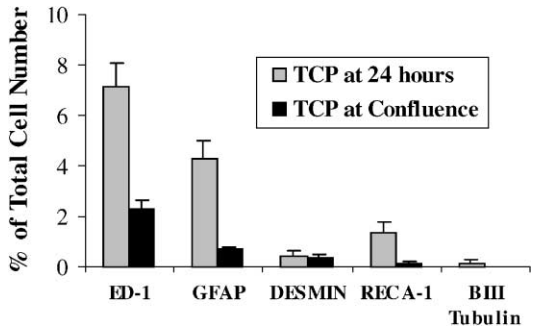

Fig. 1. The cellular composition of meningeal cultures on TCP, at 24 h, and at confluence. Using cell-specific markers, cultures were examined for the presence of other non-meningeal cell types contained within the extracted meningeal tissue. Five markers were used, including ED-1 for macrophages and microglia, GFAP for astrocytes, desmin for smooth muscle cells, RECA-1 for endothelial cells, and βIII tubulin for neurons. The number of positively labeled cells for each marker is reported as the percentage of the total cell number $\pm$ SEM.

approximately 7% of the total population. GFAP-labeled astrocytes were second highest at approximately 4%, followed by desmin positive smooth muscle cells, RECA-1 positive endothelial cells, and βIII tubulin-labeled neurons. Cells that did not stain for the cell-specific markers were vimentin positive and generally had a fibroblastic morphology, ovoid nuclei, polygonal shape and well-developed actin stress fibers (data not shown). Several distinct size classes could be distinguished under phase contrast microscopy. At confluence the percentage of fibroblasts increased, as the percent of cell-type-specific labeled cells dropped to less than 4% of the total cell number, with only ED-1 positive macrophages and microglia present above 1% of the total population, at just over 2%.

3.1.1. Meningeal ECM production on TCP

Extracellular matrix was examined on fixed cells at 48 h after plating, at confluence, and 7 days after reaching confluence with antisera against cellular fibronectin (CFN), type I collagen, and chondroitin sulfate proteoglycan (CSPG). Fig. 2 shows the expression pattern for all three proteins, with increased matrix production associated with longer time in culture. In general, cells formed thick fibrillar networks of fibronectin that covered the entire culture surface. Type I collagen increased in relative abundance over time with locally dense bundle formation. CSPG matrix expression remained diffuse and punctate, but increased in relative amount and distribution with time in culture.

3.1.2. Co-culture of neurons on meningeal cultures

Matrix deposition and meningeal cell colonization at the host/implant interface can compromise the performance of many types of implantable CNS devices. This is especially serious with bridging technology where reduced neurite outgrowth by colonization of reactive meningeal and glial cells may occur. In order to determine the effects of meningeal-coated substrates on neuron outgrowth, we co-cultured two neuronal cell types, peripheral dorsal root ganglion (DRG) neurons and central cerebellar granule neurons (CGN) on confluent meningeal cultures grown on TCP. For control model surfaces, TCP was coated with laminin for DRG neurons, and PS was coated with L1 for CGNs. Fig. 3 shows neurite outgrowth for DRG neurons and CGNs as a percent of control outgrowth on the respective model surface. When grown on the meningeal cultures, both neuronal types showed significant decreases in outgrowth when compared to control ($p<0.05$). Meningeal cultures supported peripheral DRG growth at 80% of the outgrowth on laminin-coated TCP, while neurite outgrowth for central neurons was much poorer, as CGNs measured only 33% of controls grown on the L1 adsorbed TCP.

3.2. Biomaterial characterization by contact angle and FTIR

Biomaterial-coated coverslips were fabricated by a spin-coating process as previously described [22]. The biomaterials were analyzed by surface contact angle and FTIR. Contact angle measurements reflected differences in the hydrophobic nature of the various chemistries as displayed in Table 1. In addition, FTIR analysis (data not shown) confirmed the differences in chemical identity of the various polymeric coatings employed, as previously shown [22].

3.3. Cellular composition on the biomaterials

To assess differences in cellular composition from those observed on TCP, meningeal cultures on the various biomaterials were examined 24 h after plating and upon reaching confluence. A total of 42 visual fields were counted from representative coverslips at both time points for each cell type specific marker. This method yielded average DAPI-positive total cell counts for each marker set of 1130 cells at 24 h and 8770 cells at confluence on TCP. Total cell counts on the other materials differed depending upon initial cell adhesion and proliferation rates. Surface chemistry did not appear to affect the cellular composition at 24 h, as similar cell percentages were observed for meningeal cultures on all of the biomaterials examined, with no statistical deviations from values on TCP as displayed in Table 2. Although the rate of cell growth varied, cultures readily grew to confluence within 1–2 weeks of plating on all of the surfaces, except PES, PS, and PP, which supported patchy areas of adherent cells. Cell percentages at confluence on the materials were also similar to TCP, with statistical differences only in the percentage of ED-1 positive cells. Cell populations

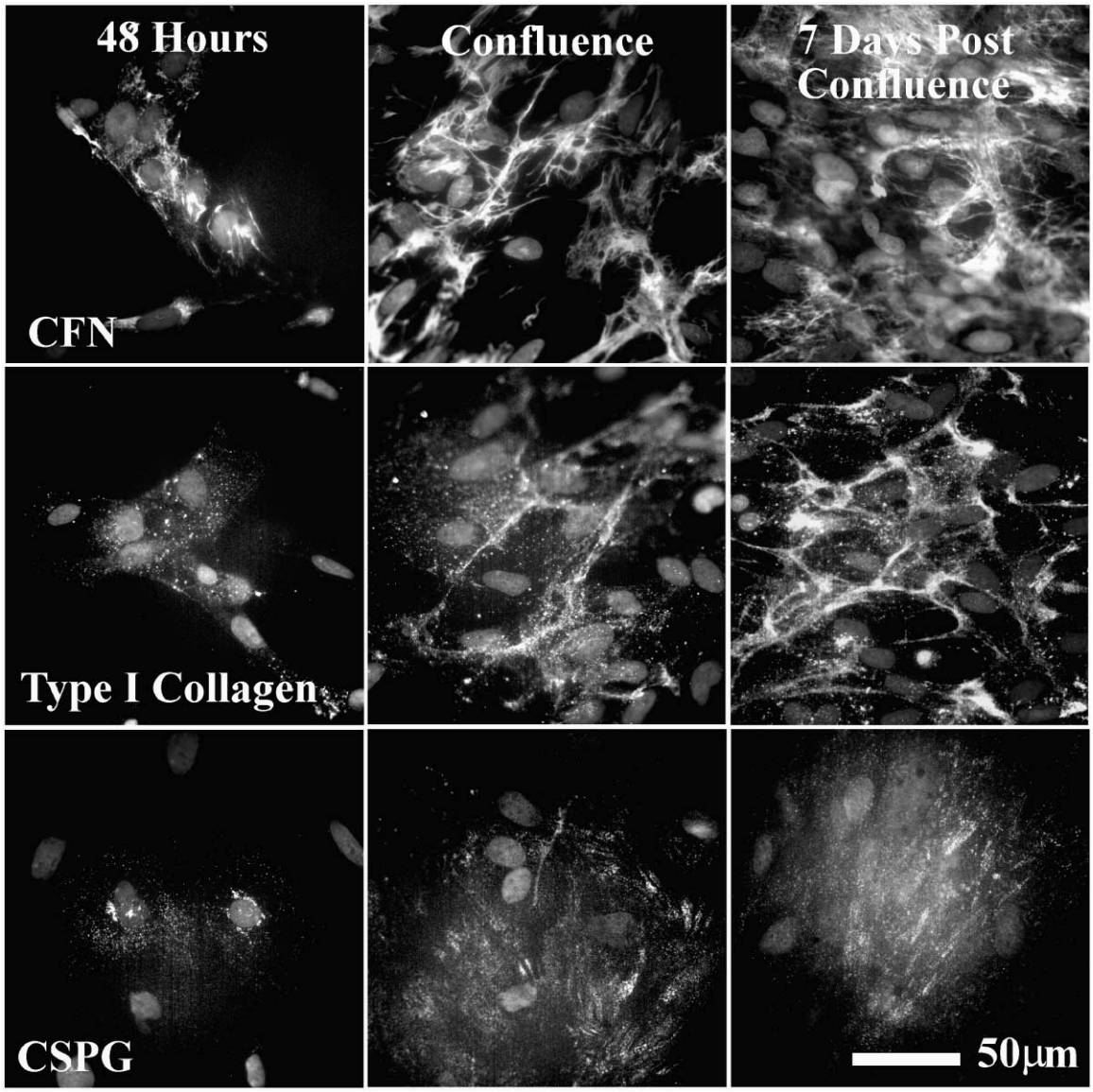

Fig. 2. Extracellular matrix expression by meningeal cultures on TCP. Cells were plated at low density, fixed after 48 h, upon reaching confluence, and 7 days after reaching confluence, then labeled for cellular fibronectin (CFN), type I collagen, and chondroitin sulfate proteoglycan (CSPG). Individual cells are distinguished by their DAPI stained, gray ovoid cell nuclei.

grown on surfaces requiring longer culture time to reach confluence than TCP (CA, TECO, PAN-PVC), showed higher percentages of ED-1 positive cells. Nonetheless, the average percentage of adherent fibroblasts on all of the materials supporting confluent growth remained at around 90% (see Table 2). Results from the two time points suggested an initial population of greater than 85% fibroblasts that increased in purity with time in culture, and which was not significantly affected by the surface chemistry of the underlying biomaterial.

3.4. Cell attachment to biomaterials

Cells were plated at a density of 5000 cells per coverslip in DMEM-FBS on the materials. Cells were incubated for 24 h, fixed in 4% paraformaldehyde, and stained with DAPI to visualize nuclei for counting. Fig. 4(A) shows the number of attached cells on the various materials listed in order of increasing hydrophobicity. Twenty-four hours after plating, a general decrease in cell adhesion was observed with increased material hydrophobicity. Attachment was significantly lower ($p < 0.05$) than on TCP for all the materials except CA. Data analysis showed statistically significant differences between groups of low (TCP and CA), moderate (TECO, PES, PAN-PVC, PEVAC), and high (PS and PP), hydrophobicity. The least hydrophobic materials supported the highest levels of cell attachment, including glass, TCP, and CA, while the more moderately hydrophobic materials of TECO, PES, PAN-PVC,

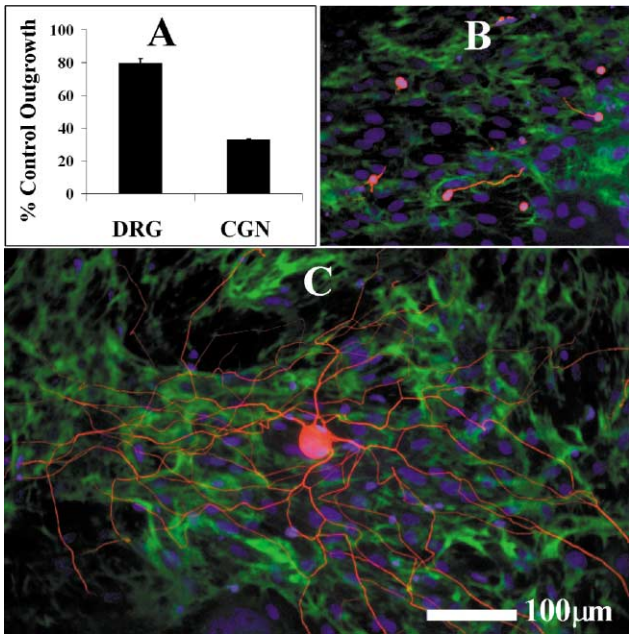

Fig. 3. Neurite outgrowth of dorsal root ganglion (DRG) and cerebellar granule neurons (CGN) cultured on confluent meningeal monolayers on TCP. (A) Neuronal outgrowth on the meningeal monolayer is reported as the percentage of outgrowth on a control surface. For controls, neurons were cultured on laminin-coated TCP for DRG neurons, and on L1-coated PS for CGNs. Neurite outgrowth for neurons in all conditions was measured after 24 h in culture. (B) CGNs on a meningeal cell monolayer. Neurons are stained in red by βIII tubulin, meningeal cells in green for the expression of cellular fibronectin, and cell nuclei are stained in blue by DAPI. (C) DRG neuron on a meningeal cell monolayer. The neuron is stained in red by βIII tubulin, meningeal cells in green for the expression of cellular fibronectin, and cell nuclei are stained in blue by DAPI.

and PEVAC supported less cell adhesion. PP and PS, the most hydrophobic materials, supported only minimal cell attachment.

3.4.1. Cell spread area and surface coverage on biomaterials

Cell spread area measurements on the various materials were taken 24 h after plating. Cells were stained with rhodamine phalloidin to visualize the actin cytoskeleton, digital images were captured, and cell spread area was calculated using computer-assisted image analysis. Fig. 4(B) shows that cell spread area on the various materials followed a similar pattern to that for cell attachment. With the exception of TECO, cell spread area decreased with increasing substrate hydrophobicity. Statistical analysis revealed the presence of three groups. TCP supported the greatest cell spread area and was statistically higher than any of the other surfaces. The second group consisted of glass, CA, PES, and PAN-PVC, and was followed by a group of TECO, PEVAC, PP, and PS, that supported the lowest cell spread area. Surface coverage measurements on

Table 1
Materials and contact angles

Material	Contact angle
Glass	35
Tissue culture plastic (TCP)	49
Cellulose acetate (CA)	52
Tecoflex (TECO)	63
Polyether sulphone (PES)	64
Polyacrylonitrile-polyvinyl chloride (PAN-PVC)	67
Polyethylene vinyl acetate (PEVAC)	75
Polystyrene (PS)	87
Polypropylene (PP)	95

TCP showed that meningeal cultures covered only 3% of the total substrate area after 24 h in cultures.

3.4.2. Cell proliferation on biomaterials

The percentage of cells undergoing division, as measured by the incorporation of BrdU into their nuclei during DNA synthesis, was used as an indicator of meningeal cell proliferation. Fig. 4(C) shows the percentages of cells incorporating BrdU, which ranged from 33% to 62%. Only division on PS and PP was significantly different from that on TCP. Cells proliferated and readily grew to confluence within 1–2 weeks on all of the materials, except PES, PS, and PP, for which only patchy growth and restricted areas of confluence were observed. At the initial plating density of 5000 cells per coverslip, the low initial cell attachment, combined with low proliferation, may account for the lack of widespread confluence on these materials.

3.4.3. ECM expression on biomaterials

The deposition of extracellular matrix by the meningeal cultures was evaluated on each material. Roughly 5000 cells were plated and cultures were fixed 48 h after plating, at confluence, and 7 days after reaching confluence, and evaluated for the expression of cellular fibronectin (CFN), type I collagen, and chondroitin sulfate proteoglycan (CSPG). Figs. 5–7 show representative images of ECM production on four representative surfaces. Although positive staining was observed for all three matrix components at the 48 h time point, compared to TCP, differences were apparent in the expression patterns on the polymers. Fibronectin expression appeared to coincide with cell spread area. Well spread cells, on the hydrophilic surfaces, displayed a more developed fibrillar matrix than cell populations growing on the hydrophobic materials. Type I collagen and CSPG were only diffusely expressed at 48 h, with no fibril formation. Matrix expression increased with time in culture for all of the materials. In general, fibronectin was expressed in thick fibrillar bundles, regardless of the underlying surface chemistry (Fig. 5). Type I collagen

Table 2
Cellular composition of meningeal cultures on materials (% of total)

	Time points 24 h and confluence	ED-1	GFAP	DESMIN	RECA-1	βIII tubulin
Glass	24 h	8.5 ± 0.82	3.0 ± 0.43	1.8 ± 0.49	1.4 ± 0.40	<0.1
	5 days	2.7 ± 0.38	0.4 ± 0.05	0.1 ± 0.03	0.2 ± 0.04	<0.1
TCP	24 h	7.2 ± 0.90	4.3 ± 0.72	0.4 ± 0.20	1.3 ± 0.42	<0.1
	5 days	2.3 ± 0.31	0.7 ± 0.10	0.4 ± 0.15	0.2 ± 0.04	<0.1
CA	24 h	4.7 ± 1.42	0.4 ± 0.19	1.4 ± 0.79	0.4 ± 0.40	<0.1
	11 days	9.5 ± 1.69	0.8 ± 0.55	0.7 ± 0.37	1.4 ± 0.66	<0.1
TECO	24 h	12.0 ± 1.82	5.1 ± 1.51	2.8 ± 1.10	0.7 ± 0.40	<0.1
	12 days	15.0 ± 2.02	2.1 ± 0.66	1.1 ± 0.37	0.7 ± 0.40	<0.1
PES	24 h	7.6 ± 2.13	1.9 ± 0.80	2.0 ± 0.86	0.6 ± 0.60	<0.1
	N/A					
PAN-PVC	24 h	5.3 ± 1.26	4.2 ± 0.79	2.8 ± 0.62	0.8 ± 0.54	0.2 ± 0.24
	8 days	10.4 ± 1.17	0.9 ± 0.21	1.0 ± 0.21	0.3 ± 0.08	<0.1
PEVAC	24 h	12.3 ± 2.13	4.0 ± 0.80	2.1 ± 0.86	0.4 ± 0.60	0.4 ± 0.10
	8 days	7.1 ± 1.91	1.2 ± 0.30	0.2 ± 0.12	0.5 ± 0.18	<0.1
PS	24 h	8.2 ± 2.28	3.9 ± 1.52	2.6 ± 1.36	1.2 ± 0.74	<0.1
	N/A					
PP	24 h	4.0 ± 1.88	2.0 ± 0.84	1.3 ± 0.73	0.7 ± 0.75	<0.1
	N/A					

and CSPG were also expressed in greater amounts at confluence (Figs. 6 and 7, respectively). In the week following confluence, a dramatic increase in matrix production was observed on all of the materials. Fig. 6 shows that type I collagen increased in relative abundance with locally dense bundle formation, whereas CSPG matrix expression remained diffuse and punctate (Fig. 7), but increased in relative amount and intensity with time in culture.

3.5. Co-culture of neurons on meningeal colonized biomaterials

When peripheral DRG neurons and central CGNs were co-cultured on meningeal monolayers on all of the materials, both neuronal types showed significant decreases in outgrowth when compared to control ($p<0.05$). Fig. 8 shows neurite outgrowth for DRG neurons and CGNs as a percent of control outgrowth on the representative model surfaces. Although outgrowth of DRG neurons on the meningeal cultures was statistically longer on glass than on PAN-PVC or PEVAC, none of the surfaces were statistically different from outgrowth on the TCP meningeal culture. Outgrowth of CGNs on the meningeal cultures did not appear to be affected by the underlying material, as statistical differences were not observed.

4. Discussion

A number of biomedical devices are being used, or are being developed, for the treatment of CNS disorders, including shunts, catheters, stimulating or recording electrodes, cell encapsulation membranes, dialysis probes, and nerve guidance devices. Many of these devices come in contact with the meninges either during surgery, where the device may penetrate the tissue, or be more permanently in contact, as for example, electrodes that are fixed to the skull and penetrate into the brain. Disruption of the meninges in such a manner is known to elicit a host reaction characterized by meningeal cell migration to the wound site, followed by the upregulation of matrix expression, and colonization of the host/implant interface [1–3,12,13]. Cell attachment and matrix deposition by reactive cells types such as meningeal fibroblasts may compromise the effectiveness of many types of implantable devices, and evidence of meningeal-related device failures have been reported in the literature [3,14–19,21].

The ability to influence cell behavior at the host/biomaterial interface may prove useful in the optimization of devices used in the treatment of CNS disorders. For example, a material surface supporting low meningeal cell adhesion may decrease or at least slow down cell-related obstruction of hydrocephalic shunts and catheters, or may improve the performance of nerve

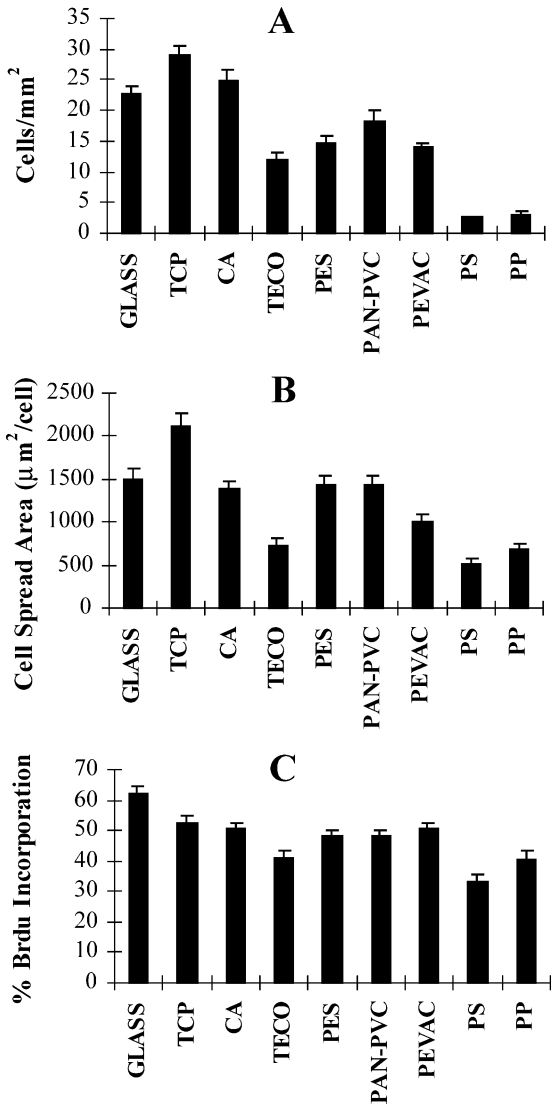

Fig. 4. Adhesion, cell spread area, and BrdU incorporation of meningeal cultures on different biomaterials. The materials are ordered from left to right as a function of increasing contact angle with water. (A) Adhesion of cells to different materials 24 h after plating. Cell number is expressed as cells per square millimeter ± SEM. (B) Cell spread area of cells of the meninges on different materials 24 h after plating. Cells were labeled by rhodamine phalloidin for visualization of their actin cytoskeleton, and spread area was measured using digital images and computer-assisted analysis. Cell area is expressed in square micrometers ± SEM. (C) BrdU incorporation by meningeal cultures. Cells were pulsed for 4 h with 10 μM BrdU prior to fixation of 48 h. Cell nuclei incorporating BrdU were visualized using an anti BrdU antibody with a fluorescently tagged secondary. The number of BrdU positive cells is expressed as a fraction of the total cells per field ± SEM.

regeneration devices by reducing meningeal colonization. Cells derived from meningeal tissues have not been studied on biomaterials, which may in part be due to the heterogeneity of cell types present and the lack of meningeal fibroblast cell type specific markers. As a menigeal culture model has not been previously described, we set out to establish a culture system using postnatal day 1 rat meningeal tissues by first examining cell type composition. Such cultures contained greater than 85% vimentin-positive, fibroblast-like cells after 24 h in culture on TCP. As the culture aged, the percentage of other cell types including neurons, endothelial cells, smooth muscle cells, astrocytes, macrophages, and microglia decreased until confluence was reached, at which time the cultures contained less than 4% of these cell types as determined by subtraction using cell type specific markers.

Meningeal cultures as initially studied covered between 3 and 5% of the various surfaces at 24 h. In general on most of the materials examined, within 8 days the cells had reached confluence and expressed a complex ECM composed of fibronectin, collagen, and CSPG. The monolayer contained intercellular contacts with abundant actin stress fibers capable of exerting tension that would cause the cell layers to contract and peel off the surface after extended time in culture. This ECM-rich, confluent culture contains similar properties to the reactive cell sheath that forms in response to injury and surrounds implanted biomaterials in the CNS.

To better characterize the effects of meningeal-derived cells on CNS-based devices, we examined the interactions of meningeal cultures with a number of medically relevant biomaterials. Cultures on the materials were first analyzed for changes in cellular composition by comparision with TCP. Overall, polymer surface chemistry did not significantly affect the percentage of cell types in adherent cultures at 24 h or at confluence. Statistical differences in cell behavior on the various materials were evident after 24 h in culture. Cell attachment and spread area decreased with increasing substrate hydrophobicity, whereas cell division was statistically lower on the most hydrophobic materials examined. Approximately 30–60% of cells incorporated BrdU suggesting that a large proportion of the cells were engaged in cell division.

Our observations of meningeal behavior as a function of substrate hydrophobicity are similar to those previously reported for other cell types. Attachment and spread cell area of fibroblasts and endothelial cells were greater on hydrophilic relative to hydrophobic surfaces with moderately hydrophobic surfaces supporting the highest levels of cell attachment [31–33]. Similar results were observed for cells grown on materials of varying hydrophobicity, and on hydrophobic gradients established on single materials. A correlation between cell spread area and proliferation has also been reported in the literature. Studies of capillary endothelial cells grown on fibronectin-coated beads and planar substrates showed that decreased cell spread area correlated with decreased proliferation and apoptosis [34]. Our data support these findings, as PP and PS, supported the lowest cell spread area and cell proliferation.

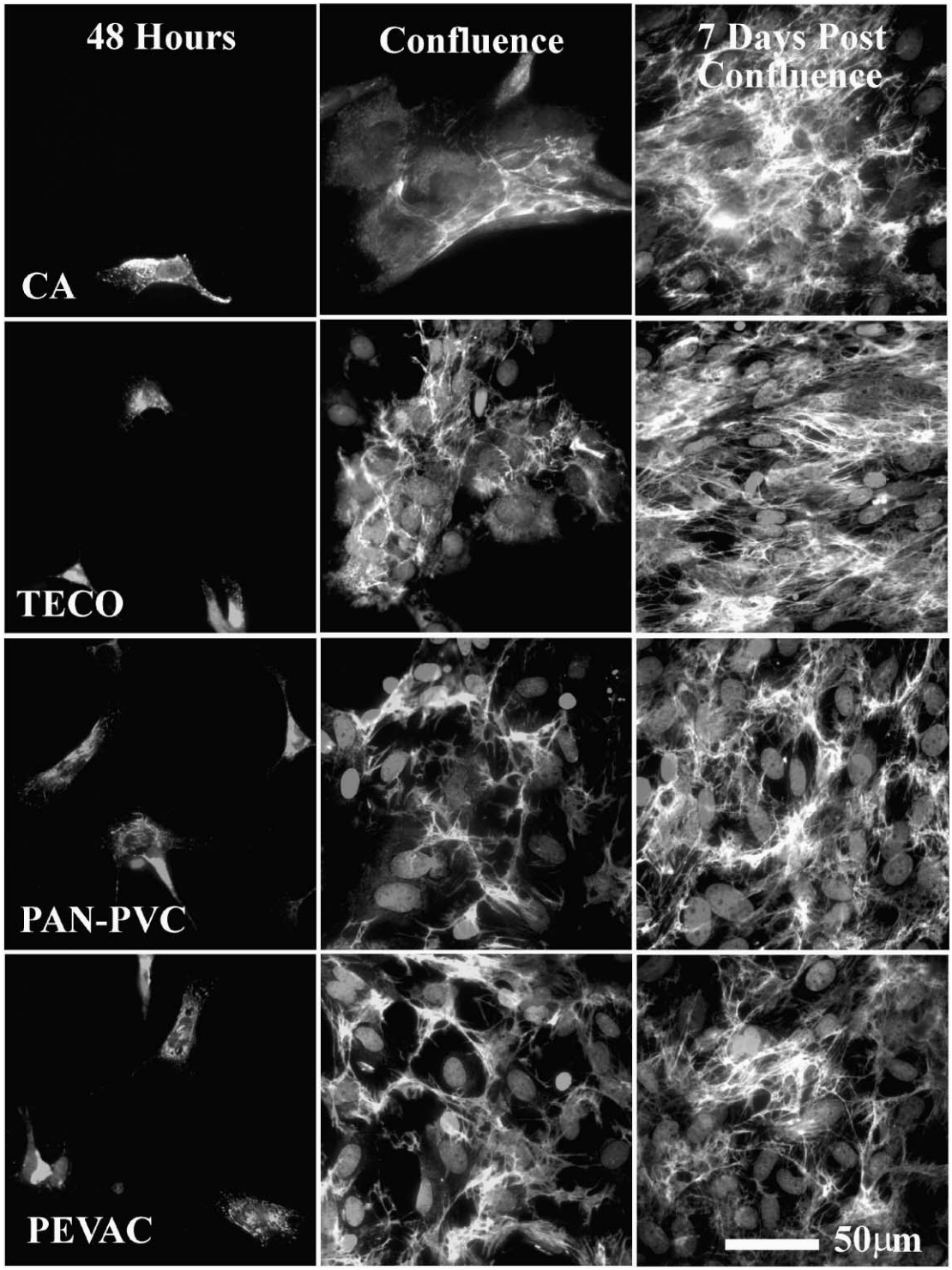

Fig. 5. Cellular fibronectin expression by meningeal cultures on selected materials at three time points. Cells were plated at low density, then fixed after 48 h, upon reaching confluence, and 7 days after reaching confluence. Cellular fibronectin is visualized using immunofluorescence. Cell nuclei, marked by DAPI, appear as gray ovals.

It is well accepted that cell interaction with materials is largely governed by the nature of the adsorbed proteins at the interface of the material. Varying levels of protein adsorption have been reported on synthetic materials [35]. For example, serum proteins such as fibronectin and vitronectin have been shown to regulate cell attachment and cell spreading [36,37]. Initially, the properties of a naive substrate direct the amount and

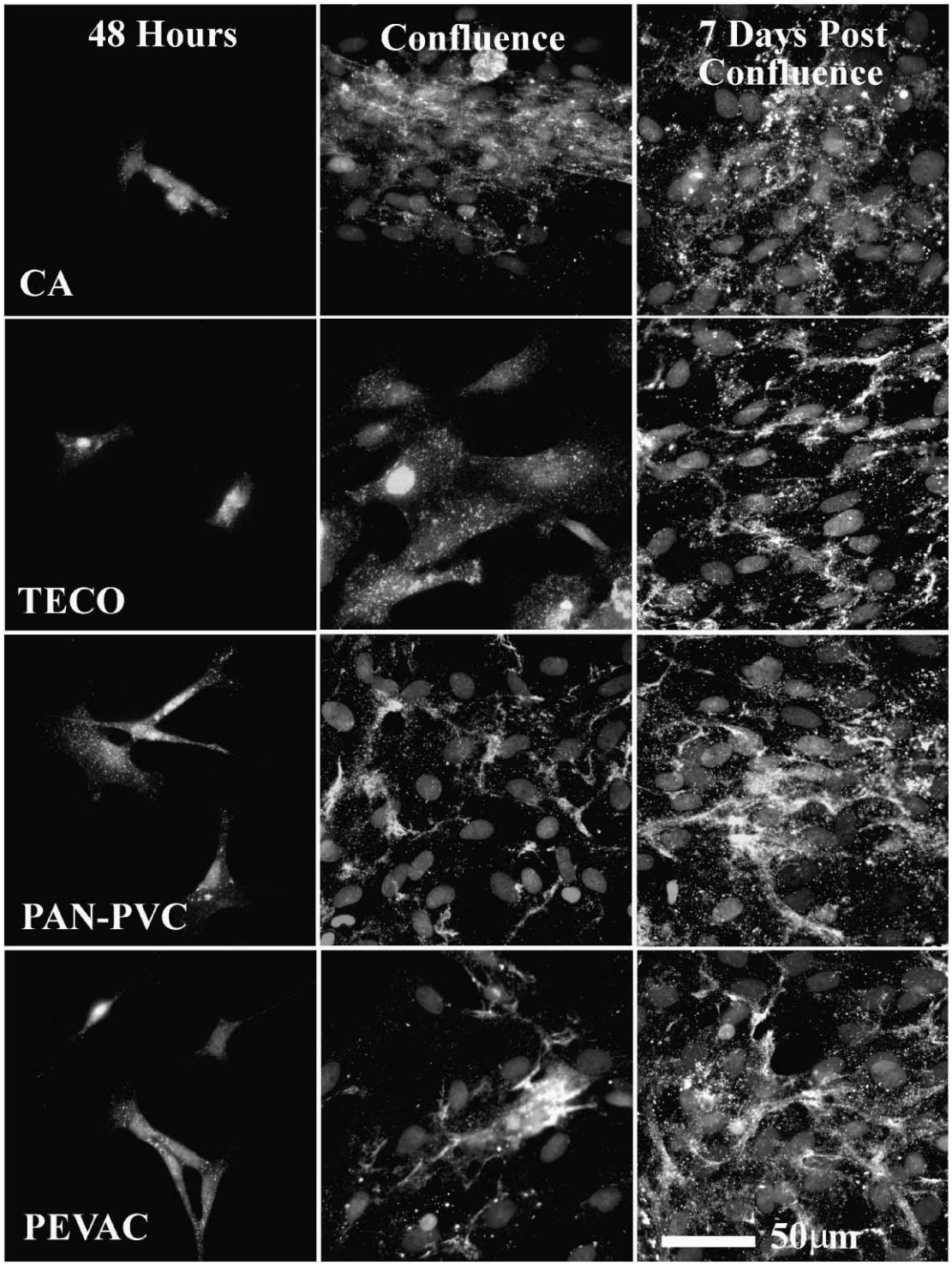

Fig. 6. Type I collagen expression by meningeal cultures on selected materials at three time points. Cells were plated at low density, then fixed after 48 h, upon reaching confluence, and 7 days after reaching confluence. Type I collagen is visualized using immunofluorescence. Cell nuclei, marked by DAPI, appear as gray ovals.

activity of adsorbed proteins [38,39]. Differences in cell behavior result from differences in amount of adsorbed proteins as well as their biological activities, which may be influenced by surface-induced conformational changes [40]. While we do not provide any direct information to support either hypothesis we suspect that each contributes to the acute differences that we observed in meningeal cell behavior.

An additional factor that can influence cells at material surfaces is the ability to modify surface proteins

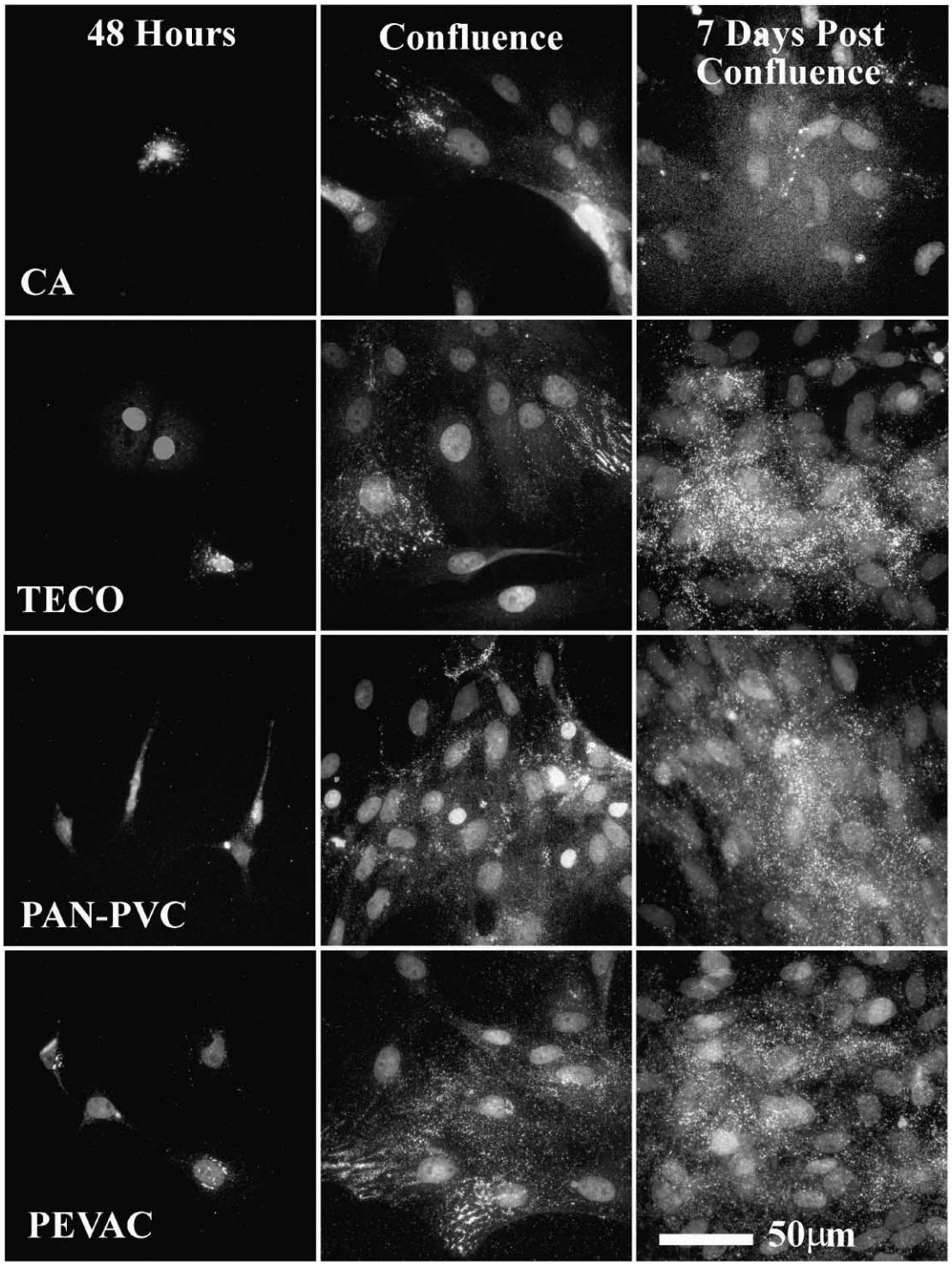

Fig. 7. Chondroitin sulfate proteoglycan (CSPG) expression by meningeal cultures on selected materials at three time points. Cells were plated at low density, then fixed after 48 h, upon reaching confluence, and 7 days after reaching confluence. CSPG is visualized using immunofluorescence. Cell nuclei, marked by DAPI, appear as gray ovals.

through secretion and remodeling of ECM. Meningeal cells express a number of ECM proteins, including fibronectin, laminin, collagen, and CSPG [23,25,41,42]. In our studies, meningeal cultures also produced a complex matrix of cellular fibronectin, type I collagen, and CSPG, irrespective of the biomaterials examined. Matrix production increased with time in culture, and culminated in the formation of a dense carpet-like network of cellular fibronectin and type I collagen, with interdispersed, punctate deposits of CSPG. Coupled

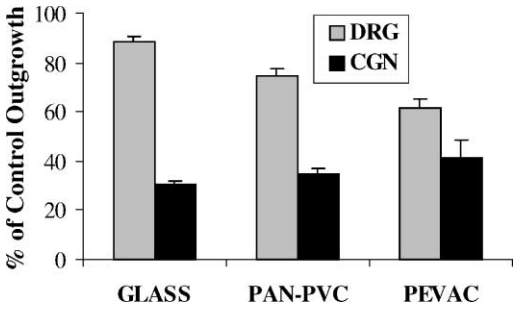

Fig. 8. Neurite outgrowth of dorsal root ganglion (DRG) and cerebellar granule neurons (CGN) cultured on confluent meningeal monolayers on selected materials. Neuronal outgrowth on the meningeal monolayers is reported as the percentage of outgrowth on a control surface. For controls, neurons were cultured on laminin-coated TCP for DRG neurons, and on L1-coated PS for CGNs. Neurite outgrowth for neurons in all conditions was measured after 24 h in culture.

with protein adsorption from the culture media, this supportive matrix enabled meningeal cells to reach confluence eventually on most of the materials, regardless of underlying surface chemistry. Meningeal cultures expanded from coverage of 3% or lower to full coverage on materials in a little over a week on average.

We used the culture system as a model to examine the influence of meningeal cells on neuronal outgrowth. Our data indicated that meningeal monolayers inhibited neurite outgrowth of both peripheral and central neurons irrespective of the chemical nature of the underlying substrate. While both neuronal cell types were inhibited by the meningeal substrate, the degree of inhibition was much greater for the centrally derived CGNs. This is likely due to cell-specific sensitivity to the secreted ECM, which is rich in fibronectin, collagen, and CSPG. While fibronectin has been shown to promote neurite outgrowth from PNS, it is not the preferred substrate for CNS-derived neurons [43], CSPG is known to inhibit growth of a wide variety of neurons, derived from both the PNS and the CNS [44].

Although meningeal cultures colonized most of the materials, temporal differences were apparent on the different substrates. Cultures reached confluence first on the least hydrophobic materials, glass and TCP (5 days), followed by PAN-PVC and PEVAC (8 days), and by CA (11 days) and TECO (12 days). Although our studies were done in vitro, our results suggest an explanation for a variety of reports involving biomaterials implanted in the CNS. It is well known, for instance, that a fibrous capsule forms around recording electrodes, which may increase impedance and eventually cause cessation of function. Turner et al. examined the cellular sheath that formed around silicon probes implanted into the cerebral cortices of rats [45]. The fibrous capsules contained numerous GFAP positive astrocytes as well as other unidentified fibroblast-like cells. The results of our meningeal cell–material interaction studies suggest that the other cells may have been cells of the meninges that colonized the probe surface perhaps to develop a glia limitans at the host/implant interface.

Previously, our group investigated the behavior of astrocytes, another important reactive component of the CNS wound healing response, on the same polymeric materials examined here [22]. As with meningeal cells, statistically significant differences were observed in initial astrocyte cell attachment and proliferation. Cell attachment decreased with increasing substrate hydrophobicity, whereas cell proliferation increased with increasing surface hydrophobicity. Astrocytes reached confluence on all the surfaces over 12 days in culture. The rate at which each population reached confluence roughly followed the same pattern as the initial differences in DNA synthesis, that is, populations with higher BrdU incorporation were the first to become confluent. Compared to meningeal-derived cells, the pattern of astrocyte behaviors on biomaterial surfaces were in large part very similar, although several differences were evident. While meningeal cells maintained a statistically similar rate of DNA synthesis on all the materials (except PS and PP, which were never fully colonized), astrocytes actually divided faster on the more hydrophobic materials, which initially supported the lowest levels of cell attachment. In addition, the rate of meningeal cell division, specifically the meningeal fibroblasts, was far higher than those reported for astrocytes under similar conditions.

Generating a unifying hypothesis on materials biocompatibility has been difficult due in large part to the myriad of experimental variables that differ between such studies. These include differences in surgical technique, site of implantation, size of implant, duration, species of animal, non-quantitative assessment of results, and varying histological techniques. Nevertheless, what can be reliably gleaned from the literature is that regardless of their composition and intended applications, most indwelling materials in the CNS elicit a characteristically similar chronic wound healing reaction. The response is invariably characterized by an elevated expression of GFAP and vimentin, the presence of microglia and foreign body giant cells, and a general thickening of the surrounding tissue that ensheaths the implant.

Our data suggests that cell type-specific differences in response to different biomaterials may play an important role in determining the ultimate nature and composition of the CNS at the host–biomaterial interface. We know that meningeal fibroblasts can attach to and grow to cover a wide range of materials. In addition, these cells secrete a rich and complex ECM that may serve to not only anchor materials within the CNS, but may decrease device performance, and is inhibitory to the growth of CNS neurons. Our results suggest that cells of the meninges present a technical

barrier to device performance and may explain the generally similar response seen following implantation of a wide range of devices that traverse the meninges. Whether indeed subtle differences will be evident in the complex environment of the injured CNS, can only be determined through studies conducted in vivo. Knowledge of both in vitro and in vivo cell–material behaviors is important in the future design of therapeutic devices used in the CNS.

Acknowledgements

The authors wish to thank Elena Budko, M.D. for her help with cell isolation. We also wish to acknowledge our funding which was provided in part by Acorda Therapeutics Inc, Hawthorne, NY, and the W.M. Keck Foundation of Los Angeles.

References

[1] Kruger S, Sievers J, Hansen C, Sadler M, Berry M. Three morphologically distinct types of interface develop between adult host and fetal brain transplants: implications for scar formation in the adult central nervous system. J Comp Neurol 1986;249:103–16.
[2] Carbonell AL, Boya J. Ultrastructural study on meningeal regeneration and meningoglial relationships after cerebral stab wound in the adult rat. Brain Res 1988;439:337–44.
[3] Rudge JS, Smith GM, Silver J. An in vitro model of wound healing in the CNS: analysis of cell reaction and interaction at different ages. Exp Neurol 1989;103:1–16.
[4] Abnet K, Fawcett JW, Dunnett SB. Interactions between meningeal cells and astrocytes in vivo and in vitro. Brain Res Dev Brain Res 1991;59:187–96.
[5] Ness R, David S. Leptomeningeal cells modulate the neurite growth promoting properties of astrocytes in vitro. Glia 1997;19:47–57.
[6] Waggener JD, Beggs J. The membranous coverings of neural tissues: an electron microscopy study. J Neuropathol Exp Neurol 1967;26:412–26.
[7] Alcolado R, Weller RO, Parrish EP, Garrod D. The cranial arachnoid and pia mater in man: anatomical and ultrastructural observations. Neuropathol Appl Neurobiol 1988;14:1–17.
[8] Nabeshima S, Reese TS, Landis DM, Brightman MW. Junctions in the meninges and marginal glia. J Comp Neurol 1975;164:127–69.
[9] Vandenabeele F, Creemers J, Lambrichts I. Ultrastructure of the human spinal arachnoid mater and dura mater. J Anat 1996;189:417–30.
[10] Rodriguez-Peralta LA. The role of the meningeal tissues in the hemato-encephalic barrier. J Comp Neur 1957;107:455–72.
[11] Feurer DJ, Weller RO. Barrier functions of the leptomeninges: a study of normal meninges and meningiomas in tissue culture. Neuropathol Appl Neurobiol 1991;17:391–405.
[12] Maxwell WL, Follows R, Ashhurst DE, Berry M. The response of the cerebral hemisphere of the rat to injury. I. The mature rat. Philos Trans Roy Soc Lond B Biol Sci 1990;328:479–500.
[13] Li MS, David S. Topical glucocorticoids modulate the lesion interface after cerebral cortical stab wounds in adult rats. Glia 1996;18:306–18.
[14] Del Bigio MR, Fedoroff S. Short-term response of brain tissue to cerebrospinal fluid shunts in vivo and in vitro. J Biomed Mater Res 1992;26:979–87.
[15] Sekhar LN, Moossy J, Guthkelch AN. Malfunctioning ventriculoperitoneal shunts. Clinical and pathological features. J Neurosurg 1982;56:411–6.
[16] Crul BJ, Delhaas EM. Technical complications during long-term subarachnoid or epidural administration of morphine in terminally ill cancer patients: a review of 140 cases. Reg Anesth 1991;16:209–13.
[17] Brown WJ, Babb TL, Soper HV, Lieb JP, Ottino CA, Crandall PH. Tissue reactions to long-term electrical stimulation of the cerebellum in monkeys. J Neurosurg 1977;47:366–79.
[18] Reynolds AF, Shetter AG. Scarring around cervical epidural stimulating electrode. Neurosurgery 1983;13:63–5.
[19] Reier PJ, Stensaas LJ, Guth L. The astrocytic scar as an impediment to regeneration in the central nervous system. In: Kao CC, Bunge RP, Reier PJ, editors. Spinal cord reconstruction. New York: Raven Press, 1983. p. 163–95.
[20] McKeon RJ, Schreiber RC, Rudge JS, Silver J. Reduction of neurite outgrowth in a model of glial scarring following CNS injury is correlated with the expression of inhibitory molecules on reactive astrocytes. J Neurosci 1991;11:3398–411.
[21] Schwab ME, Bartholdi D. Degeneration and regeneration of axons in the lesioned spinal cord. Physiol Rev 1996;76:319–70.
[22] Biran R, Noble MD, Tresco PA. Characterization of cortical astrocytes on materials of differing surface chemistry. J Biomed Mater Res 1999;46:150–9.
[23] Rutka JT, Giblin J, Dougherty DV, McCulloch JR, DeArmond SJ, Rosenblum ML. An ultrastructural and immunocytochemical analysis of leptomeningeal and meningioma cultures. J Neuropathol Exp Neurol 1986;45:285–303.
[24] Murphy M, Chen JN, George DL. Establishment and characterization of a human leptomeningeal cell line. J Neurosci Res 1991;30:475–83.
[25] Hirsch S, Bahr M. Immunocytochemical characterization of reactive optic nerve astrocytes and meningeal cells. Glia 1999;26:36–46.
[26] Duijvestijn AM, van Goor H, Klatter F, Majoor GD, van Bussel E, van Breda Vriesman PJ. Antibodies defining rat endothelial cells: RECA-1, a pan-endothelial cell-specific monoclonal antibody. Lab Invest 1992;66:459–66.
[27] Debus E, Weber K, Osborn M. Monoclonal antibodies to desmin, the muscle-specific intermediate filament protein. Embo J 1983;2:2305–12.
[28] McMenamin PG. Distribution and phenotype of dendritic cells and resident tissue macrophages in the dura mater, leptomeninges, and choroid plexus of the rat brain as demonstrated in wholemount preparations. J Comp Neurol 1999;405:533–62.
[29] Webb K, Budko E, Neuberger TJ, Chen S, Schachner M, Tresco PA. Surface bound human recombinant L1 is a selective substrate for neurons in the presence of primay astrocytes and meningeal cells. Biomaterials 2001, submitted.
[30] Takamiya Y, Kohsaka S, Toya S, Otani M, Tsukada Y. Immunohistochemical studies on the proliferation of reactive astrocytes and the expression of cytoskeletal proteins following brain injury in rats. Brain Res 1988;466:201–10.
[31] van Wachem PB, Beugeling T, Feijen J, Bantjes A, Detmers JP, van Aken WG. Interaction of cultured human endothelial cells with polymeric surfaces of different wettabilities. Biomaterials 1985;6:403–8.
[32] Williams RL, Hunt JA, Tengvall P. Fibroblast adhesion onto methyl-silica gradients with and without preadsorbed protein. J Biomed Mater Res 1995;29:1545–55.
[33] Webb K, Hlady V, Tresco PA. Relative importance of surface wettability and charged functional groups on NIH 3T3 fibroblast attachment, spreading, and cytoskeletal organization. J Biomed Mater Res 1998;41:422–30.

[34] Chen CS, Mrksich M, Huang S, Whitesides GM, Ingber DE. Geometric control of cell life and death. Science 1997;276:1425–8.
[35] Andrade JD, Hlady V. Protein adsorption and materials biocompatibility: a tutorial review and suggested hypothesis. Adv Polym Sci 1986;79:1–63.
[36] Grinnell F. Cellular adhesiveness and extracellular substrates. Int Rev Cytol 1978;53:65–144.
[37] Knox P, Griffiths S. The distribution of cell-spreading activities in sera: a quantitative approach. J Cell Sci 1980;46:97–112.
[38] Horbett TA, Schway MB, Ratner BD. Hydrophilic-hydrophobic copolymers as cell substrates: effect on 3T3 cell growth rates. J Colloid Interface Sci 1985;104:28–39.
[39] Lydon MJ, Minett TW, Tighe BJ. Cellular interactions with synthetic polymer surfaces in culture. Biomaterials 1985;6:396–402.
[40] Lewandowska K, Pergament E, Sukenik CN, Culp LA. Cell-type-specific adhesion mechanisms mediated by fibronectin adsorbed to chemically derivatized substrata. J Biomed Mater Res 1992;26:1343–63.
[41] Matthiessen HP, Schmalenbach C, Muller HW. Identification of meningeal cell released neurite promoting activities for embryonic hippocampal neurons. J Neurochem 1991;56:759–68.
[42] Sievers J, Pehlemann FW, Gude S, Berry M. Meningeal cells organize the superficial glia limitans of the cerebellum and produce components of both the interstitial matrix and the basement membrane. J Neurocytol 1994;23:135–49.
[43] Rogers SL, Letourneau PC, Palm SL, McCarthy J, Furcht LT. Neurite extension by peripheral and central nervous system neurons in response to substratum-bound fibronectin and laminin. Dev Biol 1983;98:212–20.
[44] Hoke A, Silver J. Proteoglycans and other repulsive molecules in glial boundaries during development and regeneration of the nervous system. Prog Brain Res 1996;108:149–63.
[45] Turner JN, Shain W, Szarowski DH, Andersen M, Martins S, Isaacson M, Craighead H. Cerebral astrocyte response to micromachined silicon implants. Exp Neurol 1999;156:33–49.